Light propagation in two dimensional hexagonal lattices photonic crystal

PING JIANG[a,*], KANG XIE[b], HUAJUN YANG[a], ZHENHAI WU[b]
[a]*College of Physical Electronics, University of Electronic Science and Technology of China, Sichuan Province 610054, China*
[b]*College of Optoelectronic Information, University of Electronic Science and Technology of China, Sichuan Province 610054, China*

In this work we demonstrate that light propagation in two dimensional (2D) hexagonal lattices photonic crystals (PhCs) exhibit unusual properties, such as negative refraction and preferential-direction waveguiding effects. When air-PhC interface normal is along Γ-M direction, such crystals behave as if they have a certain effective refraction index controllable by the band structure, and can be used to achieve subwavelength imaging. When the interface normal is along Γ-K direction, the propagation is allowed in the Γ-M direction. Plane wave expansion method was used to plot equal-frequency surfaces (EFCs). Finite-difference time-domain (FDTD) simulation was used to visualize wave propagation in PhC.

(Received July 14, 2011; accepted July 25, 2011)

Keywords: Effective refraction index; Negative refraction; Preferential-direction waveguide; Finite-difference time-domain simulation

1. Introduction

The phase velocity direction of the light wave propagating inside the periodical material is opposite to the energy flow. It means that the Poynting vector and wave vector are antiparallel. It gives rise to several special electromagnetic properties distinguished from conventional dielectric materials. These media are commonly known as "negative index materials" [1]. Veselago first pointed out negative refraction phenomena in 1968 [2]. Years later, several research groups have investigated left-handed-materials [3-5]. Experimental and theoretical results [6-10] indicate that negative refraction phenomena in photonic crystals are possible in regimes of negative group velocity and effective negative index above the first band near the Brillouin zone center Γ. It also founded that negative refraction can result from some special EFCs at the first band of PhC [11]. An infinitely long slab can focus all Fourier components of an image within this frequency range (both the propagation waves and the evanescent waves), and make a perfect image [12]. R. Moussa investigated the superlensing behavior in 2D PhC [13]. Cubukcu et al. demonstrated experimentally single beam negative refraction and superlensing in the valence band of 2D PhC operating in the microwave region [14]. Berrier et al. presented an experimental verification of negative refraction for infrared wavelength in an effective-negative-index PhC [15]. Zhang proposed a 2D metal-core PhC, which can achieve effective negative indexes for both TE and TM modes [16]. Lu et al. demonstrated an imaging experiment by using a slab of an effective-negative-index PhC in the microwave region [17]. Foteinopoulou et al. emphasized the time evolution of an EM wave as it hits the interface between a right-handed and a left-handed material [18].

Regarding PhC, there are two possible working regimes: a) photonic spectral bandgap: all lights inside the crystal within a certain wavelength range are forbidden; b) allowed frequencies where exhibit a wide variety of anomalous refractive effects (such as negative refraction, subwavelength imaging, superprism effect, et al). It makes controlling the flow of light in a structure becomes possible. Since PhCs are more feasible to fabricate in the optical region than negative index materials, effective-negative-index PhCs attracted tremendous interests of electrical engineers and physicists. One of the most prominent properties of effective-negative-index PhCs is that it can "amplify" evanescent waves, which can be used to achieve subwavelength imaging.

In this paper we study refraction properties of light in 2D hexagonal lattices PhC. Two different cases of air-PhC interface normal direction, including along Γ-M direction and Γ-K direction are discussed and negative refraction with effective-negative-index and preferential-direction waveguiding phenomena are investigated. Plane wave expansion method is used to solve complex eigenvalue problems. The photonic band structure curves and EFCs are plotted to find different refraction frequency ranges. FDTD simulating method is employed to visualize what has come to be known as effective-negative-index refraction.

2. Band structure in hexagonal lattice photonic crystal

In this part we consider the band structure of 2D hexagonal lattices PhC. The background material is chosen as silicon (ε=12) and the radius of the air holes is 0.4*a*, where *a* is the lattice constant. First, we employ plane wave expansion method to calculate the TM polarized (in-plane magnetic field) band curves as shown in Fig.1. It's found that a region where negative refraction occurs is in the vicinity of normalized frequency ω=0.315($2\pi c$/a) . This frequency corresponding to effective-negative-index $n_{eff}=-1$ is obtained directly by finding the second band curve intersection with the light line.

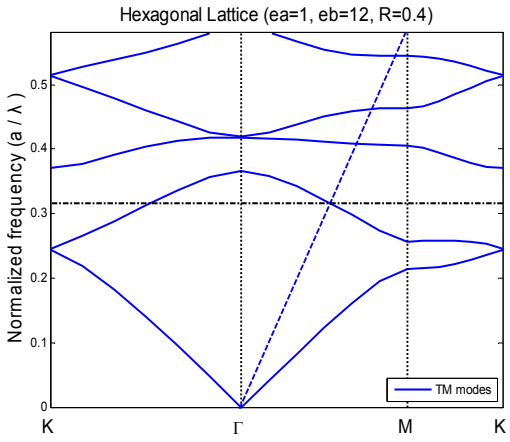

Fig.1. TM polarized band curves of the 2-D hexagonal lattices PhC with air holes of radius r=0.4a, in a silicon host matrix with ε=12. The dash line origins from Γ point represents light line. The horizontal dash line indicates normalized frequency ω=0.315($2\pi c$/a) *corresponding to the effective-negative-index* $n_{eff}=-1$.

It was demonstrated that negative refraction can result from special shape EFCs of the hexagonal lattices PhC [19]. At the second band, the EFCs can be approximated by circles close around Γ point, but become sharp corners away from Γ point. Effective-negative-index can be defined around Γ point. This kind of photonic crystal can be referred as effective negative refraction PhC. Fig.2 (b) shows the EFCs of TM mode for the normalized frequencies between ω=0.263($2\pi c$/a) and ω=0.360($2\pi c$/a) . The interval is ω=0.005($2\pi c$/a) . The high frequency contour is close to Γ point (the center of circles). The shapes of the EFCs are almost circular at the second band for a frequency between ω=0.300($2\pi c$/a) and ω=0.360($2\pi c$/a) , negative refraction may happen in this frequency range. The thick circular EFC indicates the effective-negative-index $n_{eff}=-1$ at the frequency of ω=0.315($2\pi c$/a) , which is obtained by finding the second band surface intersection with the light cone of air.

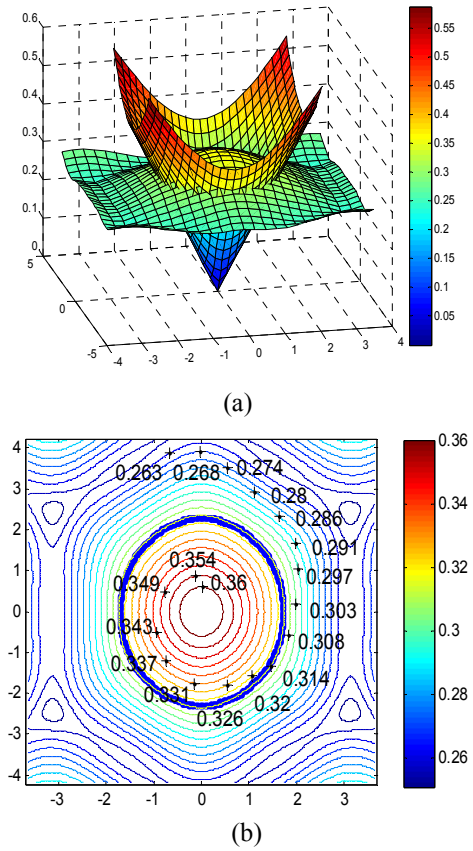

Fig.2. The TM polarized band structure and the EFCs of the second band of the 2-D hexagonal lattices PhC, frequency values are in units of 2πc/a. (a) the surfaces of second band of the PhC and the light cone, and (b) EFCs of the 2nd band. The thick circle is obtained by finding the second band surface intersection with the light cone.

3. Light refraction in hexagonal lattices photonic crystal

The refraction of light in conventional medium is determined by refractive index and Snell's law, and the range of refractive indices is limited typically between 1 < n < 3.5 in the optical frequencie. Light propagation in PhCs may behaves negative refraction near the photonic bandgaps, such crystals behave as if they have a certain effective refractive index controllable by the band structure and analogous to the effective-mass approximation in Solid State Physics [20]. Snell's law is still to be used to determine the effective refractive index which can be smaller than unity or even be negative. In this part we consider special properties when light

refraction in hexagonal lattices PhC. Two different cases of air-PhC interface normal direction will be concerned, including along Γ-M direction and Γ-K direction, negative refraction with effective-negative-index and preferential-direction waveguiding effects will be investigated. It also shows that a slab of model PhC can be used to achieve subwavelength imaging.

3.1 Negative refraction with effective-negative-index

It has shown that under TM polarization, a particular effective-negative-index $n_{eff}=-1$ can be achieved at the frequency of ω=0.315(2πc/a) because at this frequency the contour of the PhC is almost as same as that of air (the thick circle in Fig. 2 (b)). We refer this kind of PhC as effective-negative-index PhC.

Fig. 3 show the contour diagram of the case that light incidents from air into the model PhC, the air-PhC interface normal is along Γ-M direction. In the PhC, the energy velocity vector equals to the group velocity vector of the Bloch mode $\mathbf{v}_g=\nabla_k\omega$, and given the conservation of tangential wave vector. A Bloch mode denoted by A can be exited in the PhC, the group velocity vector $\mathbf{v}_g$ of the refraction light is perpendicular to the EFC at A and points to Γ point, and it gives rise to negative refraction at the interface between air and PhC.

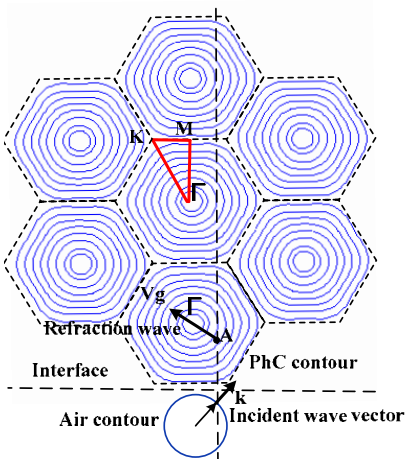

Fig.3. The EFCs plot for the PhC and air, the air-PhC interface normal is along Γ-M direction. Light wave with normalized frequency ω=0.315(2πc/a) *is launched into the model PhC, a Bloch wave denoted by A can be excited in PhC, and negative refraction can be observed. Vg is the group velocity of the Bloch wave.*

The argument to question the homogeneity and the importance of the negative refraction in a PhC with effective-negative-index is based on a simple property of the imaging configuration using a flat lens. An isotropic homogeneous medium with index of refraction $n=-1$ creates an image of a point source, the distance between the image point and the second interface of the lens varies as function of the distance between the source and the first interface, the relation illustrated directly from the simple ray diagram in Fig.4. There is no reflection at the interface between a negative index material $n=-1$ and air n=1, the coupling coefficient for any incident angle is always 100%. However, for the air-PhC interface with the PhC of $n_{eff}=-1$ (see Fig.5), results are little different.

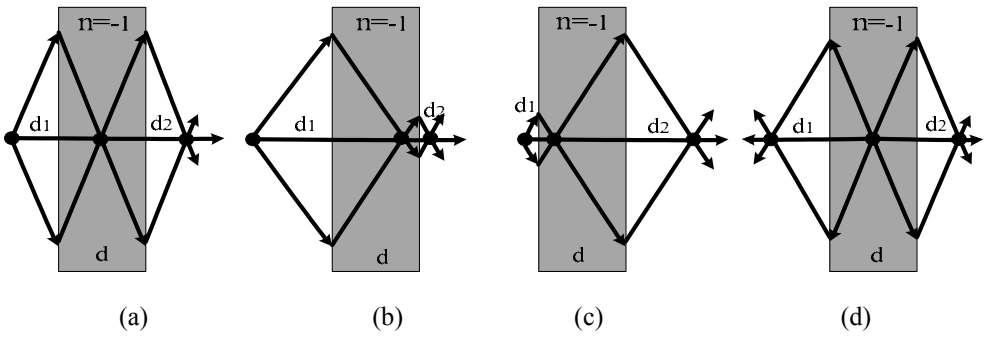

Fig. 4. The schematic illustration of the imaging effects by a flat lens made of an isotropic homogeneous medium with refraction index of $n=-1$. d_1 *is the distance between the point source and the first interface, and* d_2 *is the distance between the image point and the second interface, d is the thickness of the slab. Following four cases are discussed: (a)* $d_1=d/2$, *(b)* $d_1>d/2$, *(c)* $d_1<d/2$, *(d) source is located at center of the slab.*

An illustration of negative refraction imaging capability in PhC with effective-negative-index of n_{eff} = -1 is offered in Fig. 5. The imaging properties are as same as that of the isotropic homogeneous medium with refractive index n = -1. But reflection happens at the first interface between air and PhC slab. Incident wave cannot couple completely to the PhC. It is found that the coupling coefficient is highly angular dependent for an interface between air (n=1) and a PhC with n_{eff} = -1 [21]. This is reason why the field on the right side of the slab is slightly weaker than the filed on the left side.

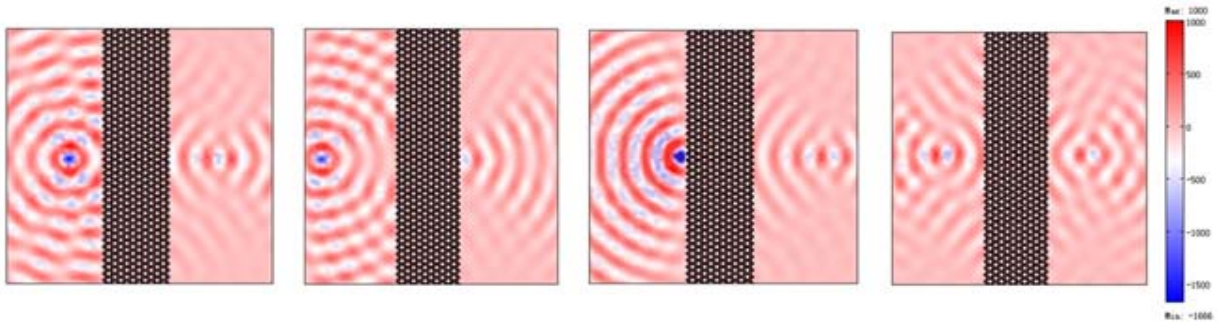

(a) (b) (c) (d)

Fig.5. FDTD simulation results of focusing a point source with a finite-width slab of 2D hexagonal lattices effective-negative-index PhC. The interface is perpendicular to the Γ-M direction and the normalized frequency is ω=0.315($2\pi c$/a) . *Assuming that the distance between the source and the first interface is equal to* d_1, *and the distance between the image point and the second interface is equal to* d_2, *the thickness of the slab is* d=5×$\sqrt{3}a$. *(a)* d_1=$d/2$, *(b)* d_1>$d/2$, *(c)* d_1<$d/2$, *(d) source is located at center of the slab.*

A similar calculation for a spherical wave starting from a point source in air (n=1) and crossing a finite-width slab of PhC with effective-negative-index n_{eff} has been done. Three different wave frequencies are simulated. For rays starting in air at a distance d_1 and angle θ_i from the first interface, using the phase Snell's law

$$\sin\theta_i / \sin\theta_p = n_{eff} < 0 \qquad (1)$$

yields the "imaging distance" f, as shown in Fig. 6, the dispersing phase and group velocities (denoted by thick and thin arrows, respectively) produce two focuses inside and outside of the slab, respectively. The FDTD simulation results shown in Fig. 7 confirm that multiple rays with different frequencies starting from a point in air can be focused by a finite-width PhC slab to different points. For the dispersive case of ω_0=0.315($2\pi c$/a) corresponding to $n_{eff} = -1$ (as the aforementioned), the image distance outside the slab presented by f_0 is equal to half of the slab thickness (the illustration and simulation counterpart results are shown in Fig. 6(a) and Fig. 7(a), respectively). Considering the frequency $\omega_1 = 0.300(2\pi c/a)$ which slightly lower than ω_0=0.315($2\pi c$/a) , the image distance f_1 is slightly shorter than f_0 , corresponding to $n_{eff} < -1$ (see Fig. 6(b) and Fig. 7(b)). For frequency ω_2=0.320($2\pi c$/a) which slightly higher than ω_0=0.315($2\pi c$/a) , the image distance f_2 is slightly longer than f_0 , corresponding to $n_{eff} > -1$ (see Fig. 6(c) and Fig. 7(c)). It found that effective-negative-index n_{eff} varies as function of the working frequencies.

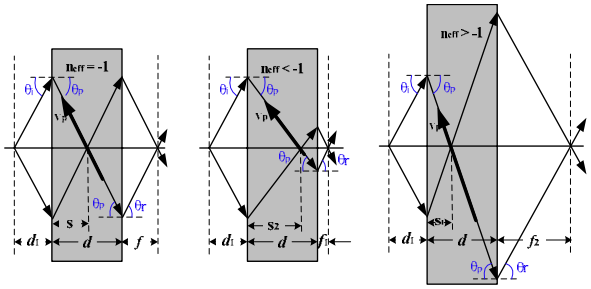

(a) (b) (c)

Fig.6. The schematic illustration of the imaging effects by a flat lens made of an effective-negative-index n_{eff} . *Thick arrow represents phase velocity and thin arrow represents group velocity. The source distance* d_1 *and the slab thickness d are fixed in following three cases: (a)* $n_{eff} = -1$, *(b)* $n_{eff} < -1$ *and (c)* $n_{eff} > -1$.

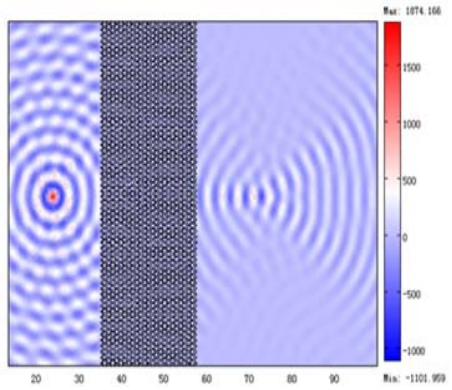

(a)

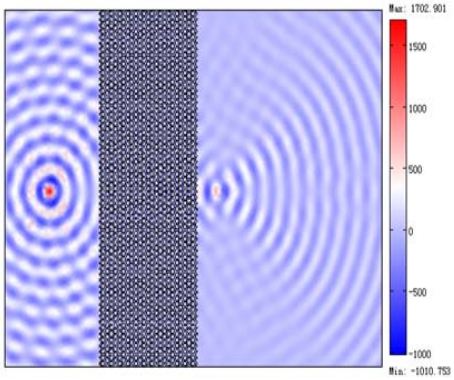

(b)

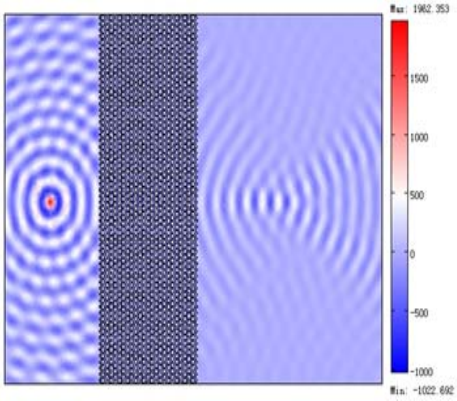

(c)

Fig. 7. FDTD simulation results of three frequencies cases of focusing a point source with a slab of 2D hexagonal lattices effective-negative-index PhC. The thickness of the slab is $d=12\times\sqrt{3}a$, *and the distance between source and the first interface is* $d_1 = d/2$. *The air-PhC interface is perpendicular to the Γ-M direction and the normalized frequencies are (a)* ω=0.315($2\pi c$/a), *(b)* ω=0.300($2\pi c$/a) *and (c)* ω=0.320($2\pi c$/a), *respectively.*

3.2 Preferential-direction waveguiding phenomena in hexagonal lattices photonic crystal

We study another situation when the air-PhC interface normal is along Γ-K direction, what will happen? The contours diagram of the light incidents from air into model PhC is shown in Fig.8 (a). It can be implied that, if the air-PhC interface normal is along Γ-K direction, a sharp corner of the EFC makes possible large changes in the direction given by the group velocity, hence a small variation of the direction of the incident wave results in two large variant direction transmitted waves in PhC. As a result, the incoming plane waves from air couples to two waves propagate in PhC along Γ-M directions. Such unusual propagation phenomena can be seems as preferential-direction waveguide.

Fig. 9 shows the FDTD simulation results of a light beam with normalized frequency of ω=0.268($2\pi c$/a) incidents into the model PhC along Γ-K direction. Two collimated beams transmit inside the PhC on both sides of the normal with refractive angle of $\pm 30^{o}$, respectively, namely in two nearby Γ-M directions.

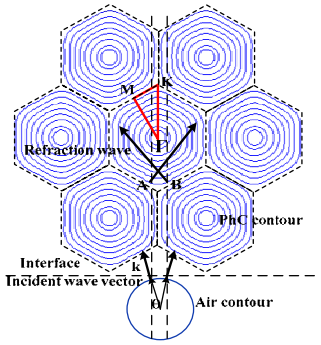

(a)

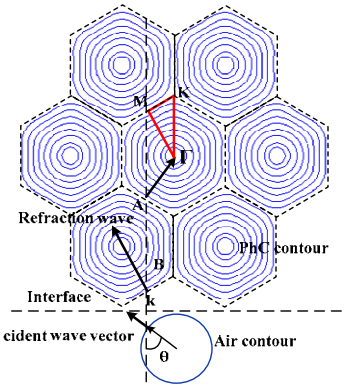

(b)

Fig.8. The EFCs plot for the TM second band of PhC and air, light waves are launched into the model PhC, the air-PhC interface normal is along Γ-K direction. A sharp corner of the EFC makes possible large changes in the direction given by the group velocity. θ is the incident angle, (a) θ is very small and (b) 0<θ<30□

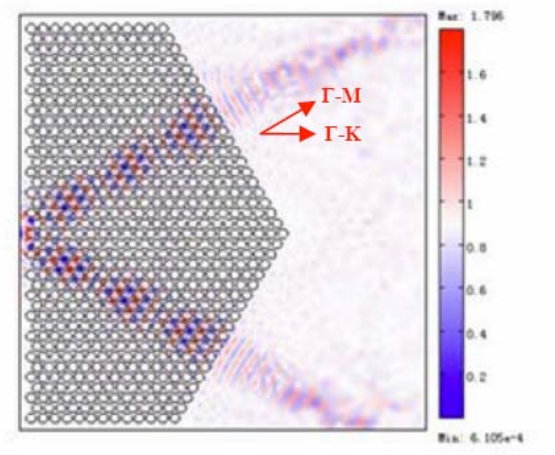

(a)

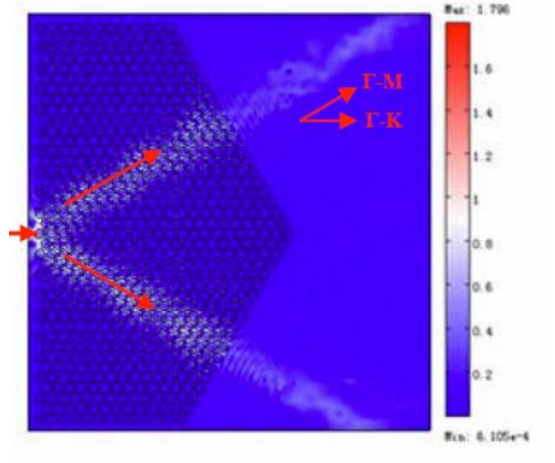

(b)

Fig.9. A plane wave with a width of a and normal frequency of ω=0.268(2πc/a) *is launched into the model PhC along Γ-K direction shows a preferential-direction waveguiding phenomena. (a) The TM field distribution and (b) light intensity distribution.*

When a light beam of ω=0.268(2πc/a) with a width of *a* and a tilt angle of θ (θ<30°) against the normal of the Γ-K direction incidents into the PhC (as shown in Fig.8 (b)). It can be observed that input light splits into two collimated beams in positive and negative Γ-M direction, respectively, as similar as normal incident case. When incident angle θ increase, light intensity in negative Γ-M direction becomes weaker and intensity in positive Γ-M direction becomes stronger (simulation result of θ=15° is shown in Fig.10 (a)). When incident angle θ reaches 30°, the light intensity in negative refraction direction almost disappeared, and the whole light transmits in the positive Γ-M direction (as shown in Fig.10 (b)).

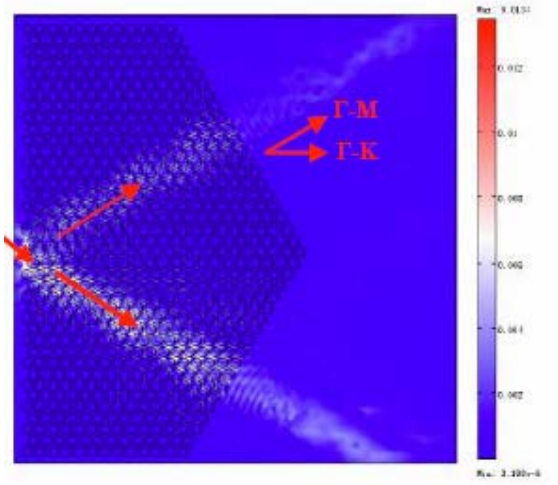

(a)

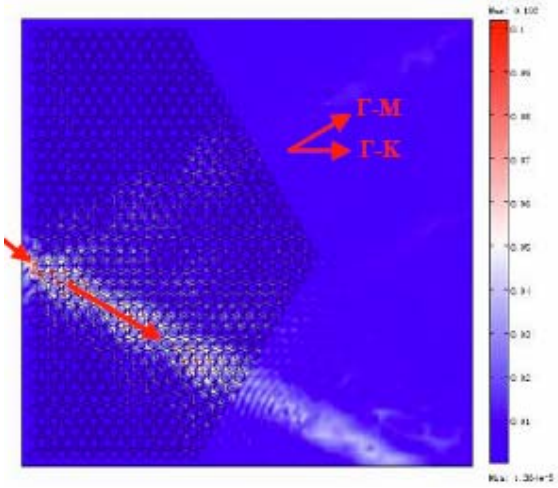

(b)

Fig.10. Light waves of ω=0.268(2πc/a) *with different incident angles are launched into the model PhC, the air-PhC interface normal is in Γ-K direction. θ is the incident angle, (a) the light intensity distribution for* θ=15° *and (b)* θ=30°

A point source is located at the center of the model PhC, the propagation is allowed in the Γ-M direction and prohibited from the Γ-K direction. The FDTD simulation result of TM field for ω=0.268(2πc/a) is shown in Fig.11. The propagation of light exhibits a preferential-direction waveguiding phenomenon in the Γ-M direction in PhC. The PhC is as same as that in Fig. 10. It clearly demonstrates the strongly anisotropic properties of such PhC for the corresponding frequencies.

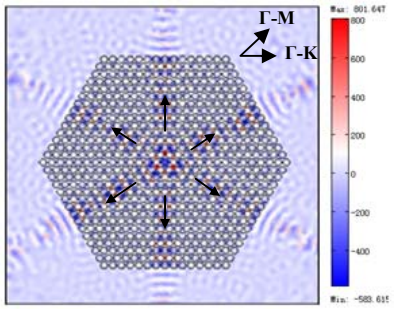

Fig.11. A point source with normal frequency ω=0.268(2πc/a) *is located at the center of the model PhC, the propagation is allowed in the Γ-M direction and prohibited from the Γ-K direction.*

4. Conclusions

In this letter we have demonstrated that different light propagation phenomena will happen when light launches from air into a PhC. If the air-PhC interface normal is along Γ-M direction, negative refraction with effective-negative-index will be observed in certain frequency range, and can be used to achieve subwavelength imaging. When air-PhC interface normal is along Γ-K direction, the propagation of light is allowed in the Γ-M direction and prohibited from the Γ-K direction, exhibiting a preferential-direction waveguiding phenomenon.

Acknowledgments

This work was supported by the National Natural Science Foundation of China under Grant No. 60588502. The author would like to express her gratitude to Professor Kang Xie and Huajun Yang for critical comments and helpful discussions. Thanks also Zhenhai Wu for PhC numerical simulations. The author would like to thank her parents and husband for understanding and spiritual support. Best wishes for her incoming baby.

References

[1] V. Veselago, L. Braginsky, V. Shklover, C. Hafner, Journal of Computational and Theoretical Nanoscience **3**, 1 (2006).
[2] V.G. Veselago, Photomagnetism, Sov. Phys USP. **10**, 509 (1968).
[3] David R. Smith, Norman Kroll, Phy. Rev. Let. **85**, 2933 (2000)
[4] Alexander A. Zharov, Ilya V. Shadrivov, Yuri S. Kivshar, Phy. Rev. Let. **91**, 3037401(2003).
[5] G. Gbur, H. F. Schouten, T. D. Visser, Appl. Phys. Lett. **87**, 191109 (2005)
[6] Zhuo LI, Binming Liang, Hanming Guo, Jiabi Chen, Songlin Zhuang, Proc. SPIE **6782**, 678210(2007)
[7] Shuai Feng, Zhi-Yuan Li, Zhi-Fang Feng, Bing-Ying Cheng, Dao-Zhong Zhang, Appl. Phys. Lett. **88**, 031104 (2006)
[8] W. Belhadj, D. Gamra, F. AbdelMalek, S. Haxha, H. Bouchriha, IET Optoelectron, **1**(2), 91 (2007).
[9] Shuai Feng, Zhi-Yuan Li, Zhi-Fang Feng, Kun Ren, Bing-Ying Cheng, Dao-Zhong Zhang, Journal Of Applied Physics, **98**, 063102 (2005)
[10] Chee Wei Wong, Rohit Chatterjeea, Kai Liua, Charlton J. Chena, Chad A. Huskoa, Proc. of SPIE **6327**, 632704 (2006)
[11] C. Luo, S.G. Johnson, J.D. Joannopoulos, J.B. Pendry, Phys. Rev., B, **65**, 201104(2002).
[12] J.B. Pentry, Negative Refraction Makes a Perfect Lens, Phys. Rev.Lett., **85**, 3966 (2000).
[13] R. Moussa, S. Foteinopoulou, Lei Zhang, G. Tuttle, K. Guven, E. Ozbay, C. M. Soukoulis, Phys. Rev. B,**71**, 085106(2005)
[14] E. Cubukcu, K. Aydin, E. Ozbay, Phys. Rev. Lett. **91**, 207401(2003)
[15] A. Berrier, M. Mulot, M. Swillo, M. Qiu, L. Thylén, A. Talneau, S. Anand, Phys. Rev. Lett., **93**(7), 073902(2004)
[16] X. Zhang, Phys. Rev. B, **71**(23), 235103(2005)
[17] Zhaolin Lu, Caihua Chen, Christopher A. Schuetz, Shouyuan Shi, Janusz A. Murakowski, Garrett J. Schneider, Dennis W. Prather, Appl. Phys. Lett. **87**, 091907(2005)
[18] S. Foteinopoulou1, E. N. Economou, C. M. Soukoulis, Phys. Rev. Lett. **90**, 107402(2003)
[19] D. Zhang, Phys. Rev. B, **70**(19), 195110(2004)
[20] Masaya Notomi, Negative refraction in phonic crystals, Optical and Quantum Electronics, **34**, 133 (2002)
[21] Zhichao Ruan, Dispersion Engineering: Negative Refraction and Designed Surface Plasmons in Periodic Structures,PHD Thesis in Microelectronics and Applied Physics Stockholm, weden, pp.31-35(2007)

*Corresponding author: jiangp@uestc.edu.cn